Journal Pre-proof

Discovery and evaluation of new compounds targeting ribosomal protein S1 in antibiotic-resistant *Mycobacterium Tuberculosis*

Yazhuang Dai, Yinqiu Xu, Chenyun Guo, Xiaowen Xue, Donghai Lin, Kejiang Lin

PII: S0223-5234(20)30286-5

DOI: https://doi.org/10.1016/j.ejmech.2020.112317

Reference: EJMECH 112317

To appear in: *European Journal of Medicinal Chemistry*

Received Date: 9 March 2019

Revised Date: 11 March 2020

Accepted Date: 6 April 2020

Please cite this article as: Y. Dai, Y. Xu, C. Guo, X. Xue, D. Lin, K. Lin, Discovery and evaluation of new compounds targeting ribosomal protein S1 in antibiotic-resistant *Mycobacterium Tuberculosis*, *European Journal of Medicinal Chemistry* (2020), doi: https://doi.org/10.1016/j.ejmech.2020.112317.

Title Page

Discovery and Evaluation of New Compounds Targeting Ribosomal Protein S1 in Antibiotic-Resistant *Mycobacterium Tuberculosis*

Yazhuang Dai[(1,3)], Yinqiu Xu[(1)], Chenyun Guo[(2)], Xiaowen Xue[(1)], Donghai Lin[*(2)], Kejiang Lin[*(1)]

(1) Department of Medicinal Chemistry, School of Pharmacy, China Pharmaceutical University, Nanjing 210009, China

(2) The Key Laboratory for Chemical Biology of Fujian Province, MOE Key Laboratory of Spectrochemical Analysis & Instrumentation, College of Chemistry and Chemical Engineering, Xiamen University, Xiamen 361005, China.

(3) Hangzhou ipharmacare Co., LTD，Hangzhou 310000, China

* Corresponding authors: Kejiang Lin & Donghai Lin

Address: 24 Tongjiaxiang, Nanjing 210009, China (Kejiang Lin);

422, Siming South Road, Xiamen 361005, China (Donghai Lin).

Email address: link@cpu.edu.cn (Kejiang Lin);

dhlin@xmu.edu.cn (Donghai Lin).

Telephone number: +86 25 83271351(Kejiang Lin);

+86 592 2186078(Donghai Lin).

The authors declare no competing financial interest.

Graphical Abstract

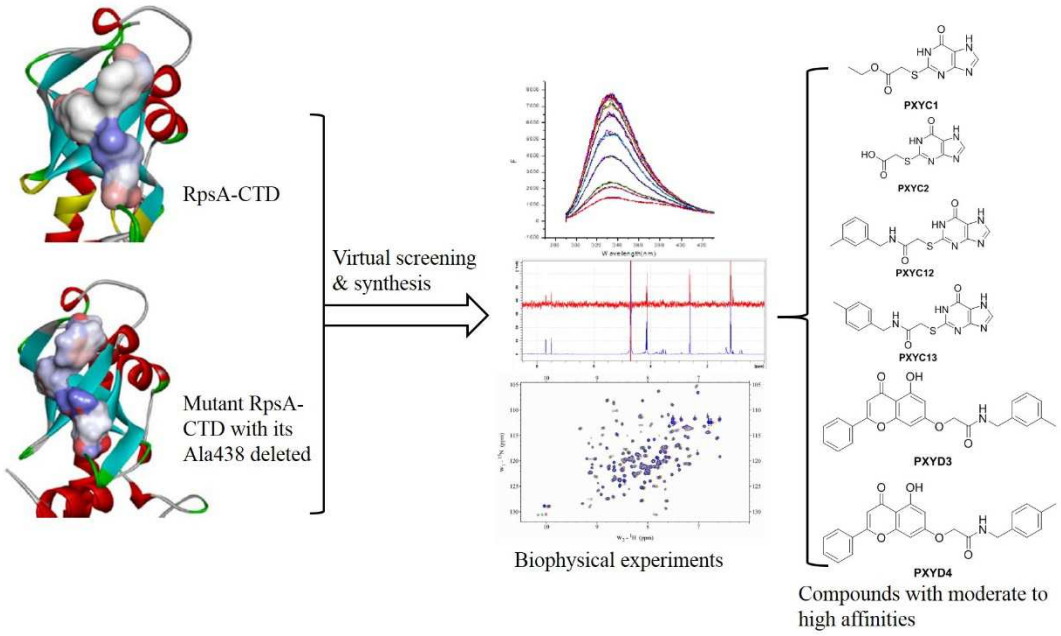

Highlights

- Based on the pyrazinoic acid binding site and an allosteric binding site, molecular docking was performed to discover potential RpsA antagonists;
- Derivatives of 2-((hypoxanthine-2-yl)thio)acetic acid and 2-((5-hydroxylflavone-7-yl)oxy)acetamide were synthesized in satisfactory yields;
- Six compounds showed good affinity to both RpsA and mutant RpsA;
- The binding sites of the active compounds are consistent with the molecular docking sites.

Discovery and Evaluation of New Compounds Targeting Ribosomal Protein S1 in Antibiotic-Resistant *Mycobacterium Tuberculosis*

ABSTRACT

The emergence of antibiotic-resistant *Mycobacterium Tuberculosis* (*Mtb*) infections compels new treatment strategies, of which targeting trans-translation is promising. During the trans-translation process, the ribosomal protein S1 (RpsA) plays a key role, and the Ala438 mutant is related to pyrazinamide (PZA) resistance, which shows its effects after being hydrolysed to pyrazinoic acid (POA). In this study, based on the structure of the RpsA C-terminal domain (RpsA-CTD) and POA complex, new compounds were designed. After being synthesized, the compounds were tested *in vitro* with saturation transfer difference (STD), fluorescence quenching titration (FQT) and chemical shift perturbation (CSP) experiments. Finally, six of the 17 new compounds have high affinity for both RpsA-CTD and its Ala438 deletion mutant. The active compounds provide new choices for targeting trans-translation in *Mtb*, and the analysis of the structure-activity relationships will be helpful for further structural modifications based on derivatives of 2-((hypoxanthine-2-yl)thio)acetic acid and 2-((5-hydroxylflavone-7-yl)oxy)acetamide.

Keywords: anti-tuberculosis agents, pyrazinamide, ribosomal protein S1, trans-translation

Introduction

Antibiotic resistance is urging new strategies to treat bacterial infections, of which tuberculosis is the leading cause of death around the world[1]. Recently, the inhibition of the trans-translation process of bacteria appears to be an effective strategy, and compounds targeting this process show broad-spectrum antibiotic activity[2]. Compounds affecting the trans-translation process of *Mycobacterium Tuberculosis* (*Mtb*) have also been discovered[3, 4], showing that the trans-translation process is a viable target for developing anti-tuberculosis drugs.

In the trans-translation process of *Mtb*, the ribosomal protein S1 (RpsA) plays an important role. As shown in Figure 1, *Mtb* initializes the process to release the stalled ribosome when stimulated by factors such as stress and mRNA damage[5]. With other molecules, such as the small protein B (smpB) and the elongation factor thermo unstable (EF-Tu), RpsA helps replace mRNA with tmRNA, which contains the information that the protein being produced is incomplete. After translation, the incomplete protein has a tmRNA-encoded peptide label, which helps with the targeted proteolysis of the protein. Without the trans-translation process, the incomplete protein may be toxic to the *Mtb* cell. Additionally, this process also ensures that *Mtb* can successfully synthesize proteins that are indispensable for survival in adversity[6].

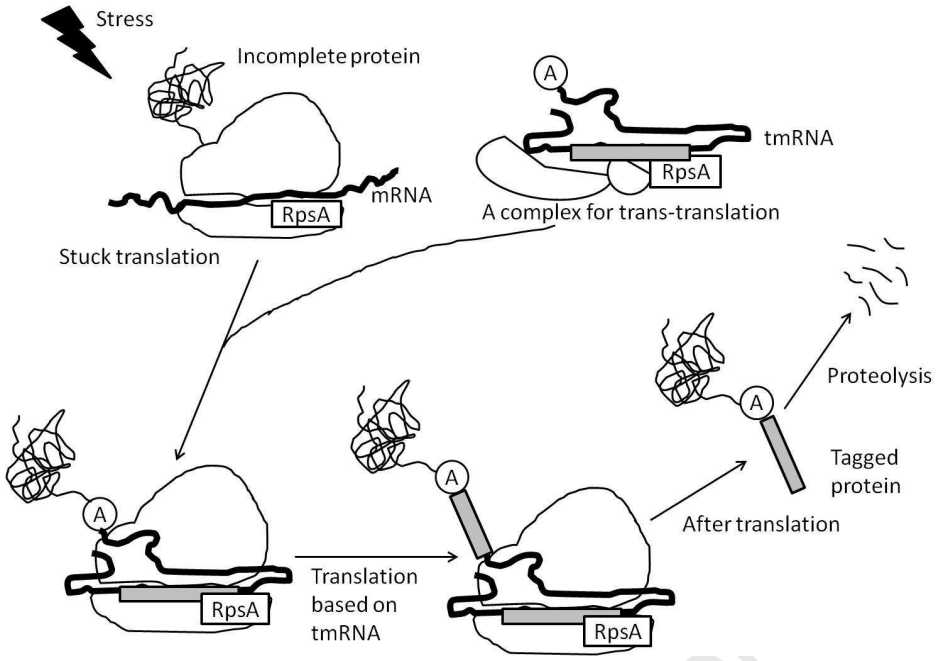

Figure 1. The role of RpsA in trans-translation. Trans-translation helps *Mtb* degrade incomplete proteins which may be toxic. The grey rectangles in the figure represent information that the protein needs to be degraded. The grey rectangle in tmRNA is an RNA sequence, and the grey rectangle in the protein is an amino acid sequence.

Pyrazinamide (PZA), a first-line anti-tuberculosis drug, plays an important role in the treatment of *Mtb* infections, and it is also related to RpsA. Among the first-line anti-tuberculosis drugs, PZA has the irreplaceable function of shortening the treatment period, even though there are several new drug candidates in clinical development [7]. These drug candidates, including the highly potent TMC207, must be used with PZA, and any combination of drugs without PZA is unsatisfactory[8-11]. PZA acts as pyrazinoic acid (POA), the product of pyrazinamidase

hydrolysis. Research suggests[12] that POA forms a complex with the C-terminal domain of RpsA (RpsA-CTD) to interfere with trans-translation, and RpsA-CTD with Ala438 deleted (RpsA-CTD Δ438A) has weak affinity for POA. Meanwhile, mutants of RpsA are phenotypically associated with PZA-resistant *Mtb*[13-15]. By performing molecular dynamic simulations, researchers found that RpsA mutants without A438, key amino acids including Phe307, Phe310, Arg355 and Arg357 are too flexible to bind POA, which could cause the PZA resistance problem[14, 16]. To discover better drugs for treating *Mtb* infections, further drug design not only needs to depend on wild type RpsA, but also should consider the flexible RpsA A438 deletion mutant, as well, so that the trans-translation process in both *Mtb* and PZA-resistant *Mtb* can be inhibited effectively.

In our previous work, we found that a barrel of the RpsA-CTD composed of β-strands shows strong affinity for RNA[17]. It is also the β-strands that approach POA in the complex structure (PDB code: 4NNI). These help drug design by showing the potential binding sites of RpsA-CTD and RpsA-CTD Δ438A. Meanwhile, trans-translation is a unique physiological mechanism of microorganisms. Therefore, targeting RpsA for drug design should have good specificity[18]. More importantly, the PZA-resistance problem is mainly caused by mutations in *pncA* gene

encoding pyrazinamidase[19]. Although PZA is a prodrug which is converted to POA by pyrazinamidase, the interaction between POA and RpsA does not rely on the activity of pyrazinamidase. Design of new compounds directly interacting with RpsA avoids the conversion process, which indicates that targeting RpsA could be an effective solution to the PZA-resistance problem.

This research focuses on the β-strands of RpsA-CTD and RpsA-CTD Δ438A to design novel inhibitors of RpsA. Molecules were selected from the docking results and synthesized. Then, saturation transfer difference (STD) was used to preliminarily evaluate the effects of the compounds, followed by the determination of dissociation constants with fluorescence quenching titration (FQT). Finally, chemical shift perturbation (CSP) was applied to show the binding sites of the active compounds.

Results and discussion

Virtual screening and synthesis

To discover molecules having effects on both RpsA-CTD and RpsA-CTD Δ438A, both the complex structure of POA with RpsA-CTD (PDB code: 4NNI) and the structure of RpsA-CTD Δ438A (PDB code: 4NNG) were used for virtual screening. According to the complex structure shown in 4NNI, the basic Arg357 inside the binding site of RpsA-CTD can form an

electrostatic interaction with the acidic POA. This suggests that Arg357 should be protonated before molecular docking. Meanwhile, the scoring functions used are more reliable than what was used before[4]. The re-docking results show that the protonated model had a smaller deviation between the docked POA and the POA in 4NNI (Figure 2a). At the same time, the protonated model distinguished between POA and PZA more clearly with the scoring functions shown in Figure 2b, which explains the fact that PZA is inactive before being hydrolysed. Based on these results, we screened new compounds with the protonated Arg357 model.

(a) (b)

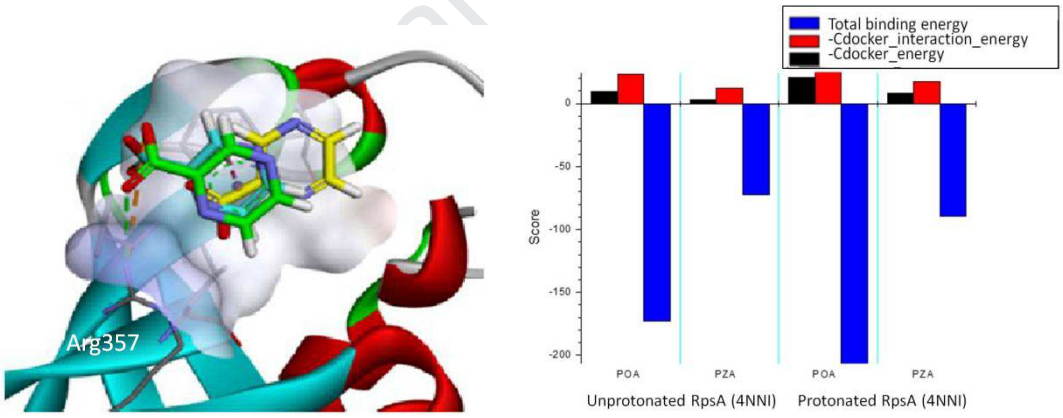

Figure 2. Re-docking results of POA. (a) Results from the protonated and the unprotonated models. POA in the complex structure is in green, while the docked poses of POA based on the protonated and the unprotonated models are in cyan and yellow, respectively. (b) Results described with three functions. The difference between the total binding energy values of POA and PZA is higher with the Arg357 protonated, and the difference of

the -CDocker_energy values is also more obvious.

After virtual screening based on RpsA-CTD and RpsA-CTD Δ438A, 2,500 compounds were retained for the binding site around the β-strands, which might be new solutions for PZA-resistance. In our previous work, ZRL15 showed the best affinity[4], and therefore, the PXYC series of compounds were selected due to their shared 2-((pyrimidine-2-yl)thio)-acetyl moiety (Figure 3). Another reason for selecting the PXYC series is that their hypoxanthine moiety resembles the purine of an RNA molecule, which has a high affinity for RpsA. From the docking results of an allosteric binding site, flavone derivatives were tentatively selected, which comprise the PXYD series.

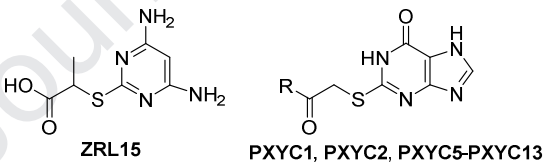

Figure 3. Similarities between ZRL15 and the PXYC series. ZRL15 has dissociation constants of 2.67 μM and 1.74 μM with RpsA-CTD and RpsA-CTD Δ438A, respectively.

As shown in Scheme 1, the 2-thioxanthine core (PXYC3) was obtained in five steps in satisfactory yield, and the functionalization of the 2-thioxanthine brought about the PXYC series. The condensation

between thiourea and ethyl cyanoacetate yielded 6-amino-2-mercaptopyrimidin-4(3H)-one (1), in which 5H was further substituted with a nitroso. The substituted product (2) was then deoxidized to obtain compound 3. A carbon was introduced to 3 through the alkanoylation of the reduced amino to obtain 4. The intramolecular condensation of 4 gave the 2-thioxanthine core.

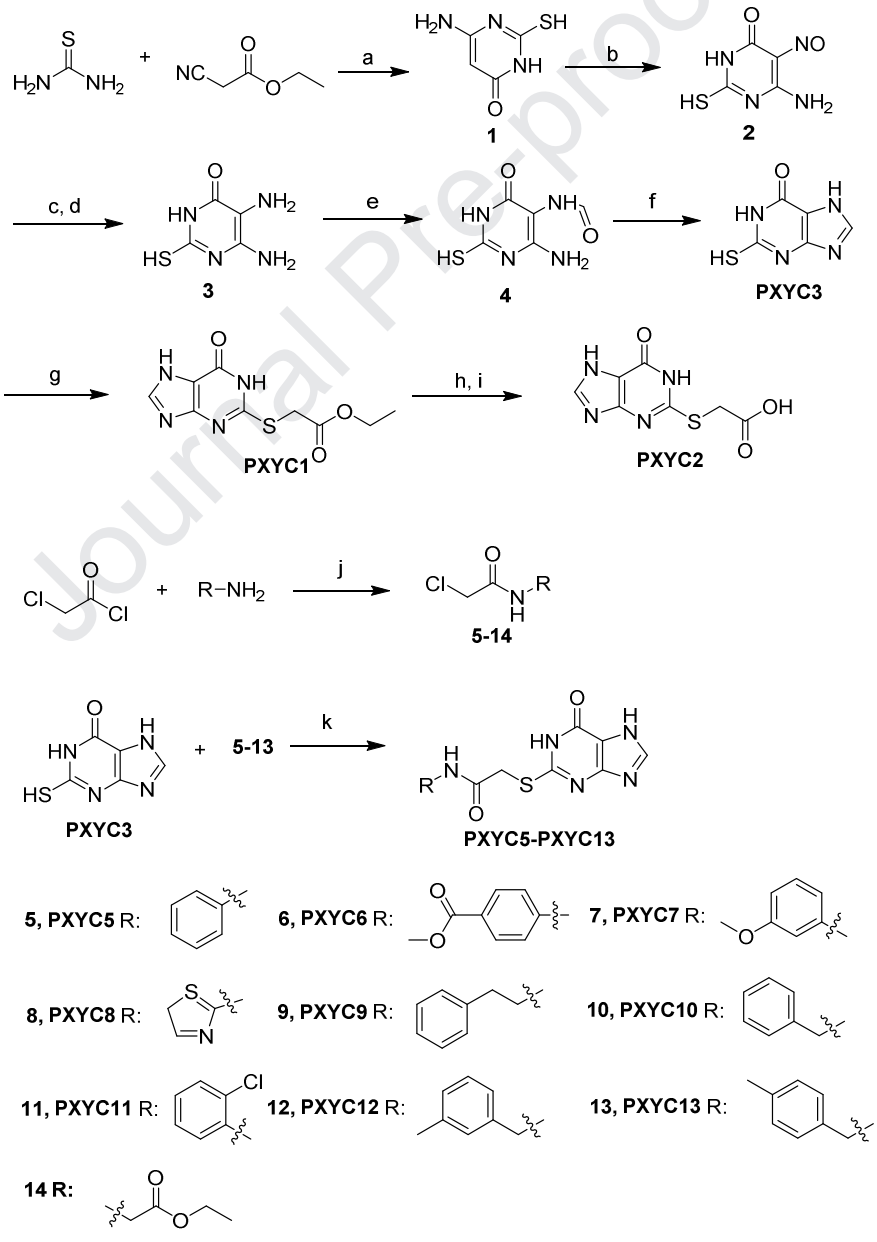

Scheme 1. Synthesis of the PXYC series of compounds. Reaction conditions: (a) EtONa, 2 h, 75 °C; (b) $NaNO_2$, H_2O, AcOH, 20 h, room temperature; (c) $Na_2S_2O_4$, $NaHCO_3$, 7 h, 0 °C; (d) AcOH, pH = 5; (e) HCOOH, 2 h, 101 °C; (f) formamide, 2 h, 178 °C; (g) ethyl chloroacetate, H_2O, 70 °C; (h) 1 M NaOH, 70 °C; (i) AcOH; (j) Et_3N, DCM, 0 °C to room temperature; (k) Et_3N or K_2CO_3, EtOH, 50 °C or room temperature.

During the functionalization of the 2-mercapto of PXYC3, the direct introduction of completed side chains had higher yields than stepwise elongations. PXYC1 was first prepared by the alkylation of the 2-mercapto with ethyl chloroacetate, and the hydrolysis of PXYC1 brought PXYC2. However, direct amination reactions of PXYC1 gave many side products. Meanwhile, the condensation between PXYC2 and the corresponding amines under HBTU and HATU catalysis had low yields. To overcome these obstacles, the completed side chains were introduced directly, which were obtained by the alkanoylation of the corresponding amines with chloroacetyl chloride. Then, the alkyl chloride products (5-13) were used to prepare PXYC5-PXYC13.

PXYD1-PXYD5 have the same side chains as some compounds in the PXYC series, so some alkyl chloride products mentioned above can also be used. As shown in Scheme 2, PXYD1-PXYD5 were directly prepared

with 5,7-dihydroxyflavone as the core. An intramolecular hydrogen bond can form between the 4-one and the 5-hydroxyl, which provides regioselectivity for the alkylation of the 7-hydroxyl.

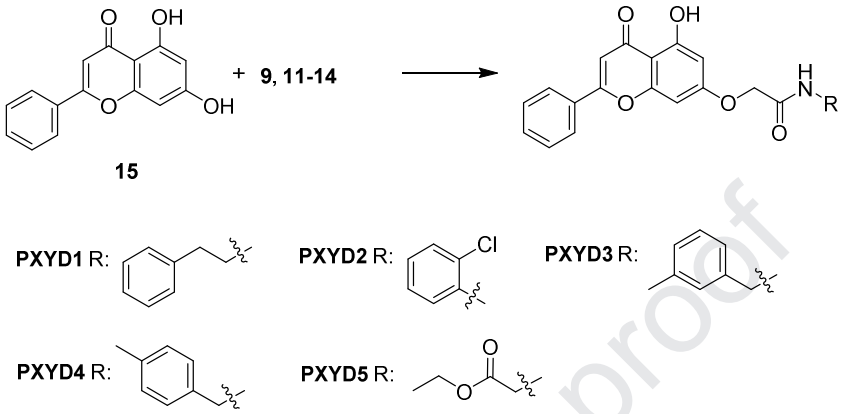

Scheme 2. Synthesis of the PXYD series compounds. Reaction conditions: K_2CO_3, DMF, 80 °C.

Preliminary tests with STD

The STD experiment is a fast method for identifying hit compounds[20], which has been widely applied to ligand-based drug design[21-23]. After the selective irradiation saturation of a receptor, the saturation can be transferred to its nearby ligand, and their spin system will try to return to equilibrium. Due to the different relaxation pathways of the system, the net spin populations belonging to the ligand may increase or decrease, which is represented as higher or lower ligand peaks on its spectrum. Based on the principle of STD, the satisfactory results preliminarily showed that the drug design was successful.

For both RpsA-CTD (285-476) and RpsA-CTD Δ438A (285-476), STD experiments were performed to test if they interact with the compounds. As shown in the difference spectra (Figure 4), PXYC1, PXYC2, PXYC12, PXYC13, PXYD3 and PXYD4 have positive signals with both RpsA-CTD and RpsA-CTD Δ438A.

(a)

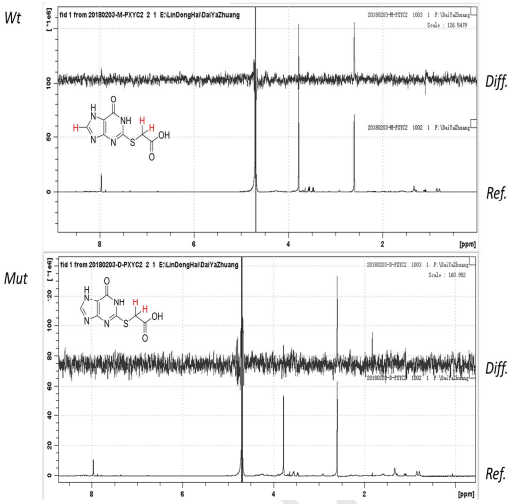

(b)

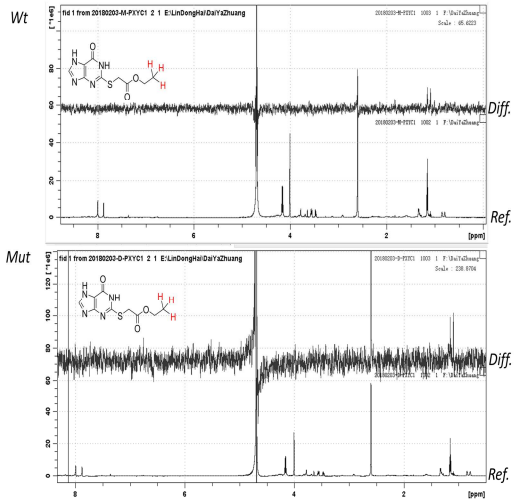

(c)

(d)

(e)

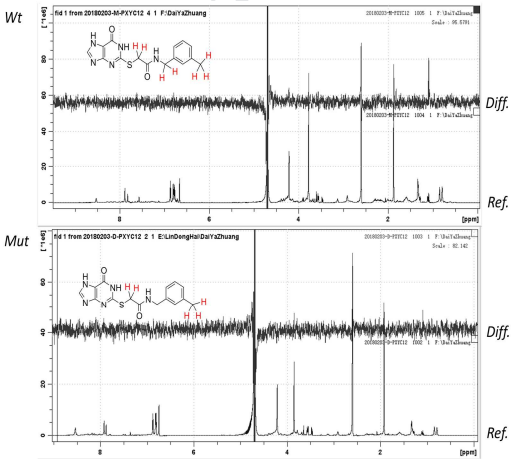

(f)

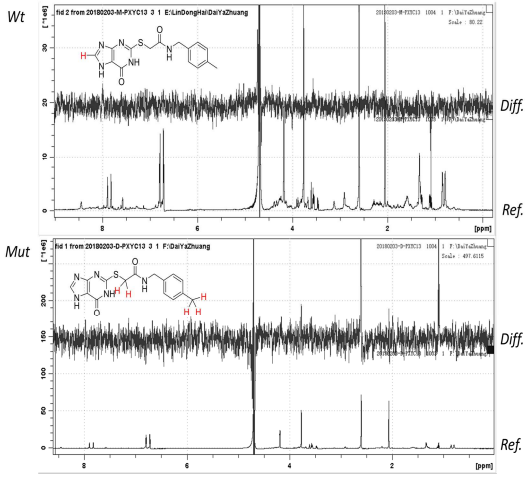

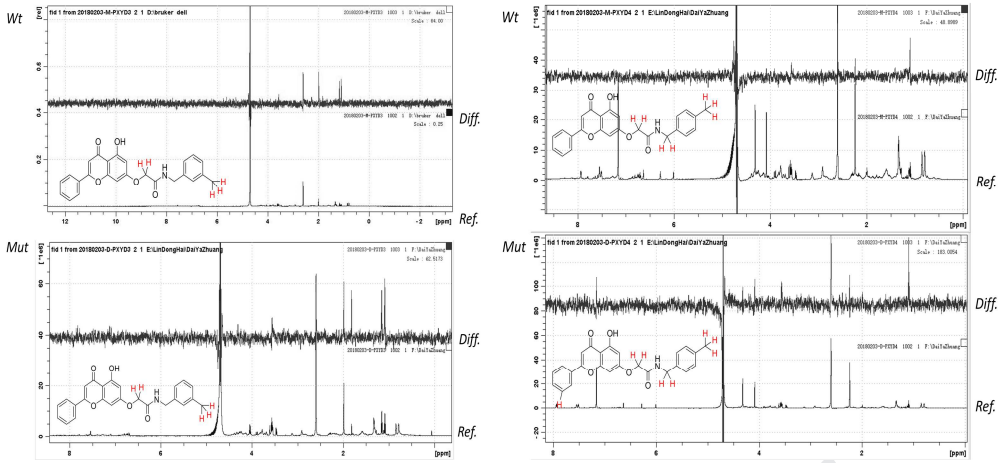

Figure 4. Results of the STD experiments. The hydrogens showing signals on the difference spectra are labelled in red. *Diff.* and *Ref.* in the figure represent difference spectra and reference spectra, respectively. *Wt* and *Mut* stand for RpsA-CTD and RpsA-CTD Δ438A, respectively. (a-f) Spectra of PXYC1, PXYC2, PXYC12, PXYC13, PXYD3 and PXYD4, respectively.

Determination of dissociation constants with FQT

FQT experiments can be used to conveniently evaluate the interactions between biomacromolecules and small molecules[24, 25]. The quenching rate constants (K_q) and dissociation constants (K_d) of the active compounds screened by STD are shown in Table 1. According to the Stern-Volmer equation[26], all the K_q values of the compounds are greater than $2 \times 10^{10}\ M^{-1}\ sec^{-1}$, which show that their quenching process is static rather than dynamic. Namely, the compounds have specificity for their targets. According to the number of binding ligands fitted by the

double logarithm regression curve[27], each active molecule combines with one target, which also supports the specificity of the interactions between the compounds and their targets. The K_d values fitted by the double logarithm regression curve show that all the active compounds have a stronger affinity to RpsA-CTD than POA. Notably, the K_d values of PXYC1 with the both targets are less than 1 μM, which shows that PXYC1 has the best affinity among the compounds reported in this work and our previous work[4]. In our previous work[4], compounds with moderate affinity to RpsA-CTD and RpsA-CTD Δ438A show satisfying results in drug susceptibility assays. Therefore, the performance of PXYC1 in biological tests is worth expecting. Additionally, six compounds show comparable affinity to RpsA-CTD Δ438A, which indicates their potential in antibiotic-resistance *Mtb* infections.

Table 1. Results of the FQT experiments

Compound	Target	Stern–Volmer equation Adj. R^2	K_q (M^{-1} sec^{-1})	Hill equation Adj. R^2	K_d (μM)
PXYC1	RpsA-CTD	0.989	3.37×10^{12}	0.997	0.81
	RpsA-CTD Δ438A	0.976	3.40×10^{12}	0.997	0.31
PXYC2	RpsA-CTD	0.993	1.79×10^{12}	0.986	6.35
	RpsA-CTD Δ438A	0.990	1.91×10^{12}	0.997	5.11
PXYC12	RpsA-CTD	0.976	3.75×10^{12}	0.991	2.67
	RpsA-CTD Δ438A	0.995	2.54×10^{12}	0.998	4.67
PXYC13	RpsA-CTD	0.977	4.09×10^{12}	0.956	7.61
	RpsA-CTD Δ438A	0.998	3.68×10^{12}	0.994	8.50
PXYD3	RpsA-CTD	0.992	1.94×10^{12}	0.943	5.66
	RpsA-CTD Δ438A	0.994	2.33×10^{12}	0.986	6.91
PXYD4	RpsA-CTD	0.997	6.45×10^{12}	0.992	3.24

	RpsA-CTD Δ438A	0.989	6.64×10^{12}	0.996	1.64
POA	RpsA-CTD	0.994	8.22×10^{11}	0.995	9.65

Analysis of Structure-activity relationships based on STD and FQT

STD has shown its advantages in fragment-based drug design[23]. Because the saturation of proteins can only propagate to fragments within a certain distance, fragments that are close to the protein show signals. These fragments can be important scaffolds for further structural modifications. Combined with the K_d values given by FQT, SAR can be analysed for the active compounds.

For the PXYC series, appropriate side chains attached to the 2-mercapto moiety are important. Most PXYC series difference spectra show signals belonging to methyl and methylene groups, indicating the importance of the side chains. Similarly, PXYC3 shows no activity without a side chain. An acetic acid chain brings moderate activity, whereas its ethyl esterification product shows the best affinity. It seems that both hydrophilic and hydrophobic chains can bring moderate affinity. Because the binding site for which the PXYC series was designed is a surface rather than a cavity, the hydrophobicity of the side chain may not be important. Because the ester or acylamide derivatives of PXYC3 show activity, hydrogen bond acceptors are indispensable. For the acylamide derivatives, the distance between the amide and an aryl group has the

greatest influence on activity, from which it can be inferred that around the binding site there may be an amino acid containing an aryl group. Within the distance of one carbon, a π-π interaction may form. However, this interaction looks unnecessary as the affinity of the acylamide derivatives did not exceed PXYC1, which may be due to the flexibility of the amino acid aryl group. This one carbon distance also affects the activity of the PXYD series, but the hydrophobicity of the aryl groups might be responsible for maintaining the affinities of PXYD3 and PXYD4, as PXYD5 shows no signal with STD, which has an ester extension rather than an aryl group.

Validation of binding sites with CSP

CSP has been a successful method in fragment-based drug design since the proposal of "SAR by NMR"[23, 28]. The binding of ligands changes the environment of nearby amino acids, which results in the change in peak shifts belonging to these amino acids. Based on the assignment of RpsA 280-438 which has been reported[29], the binding sites of the active compounds on RpsA-CTD can be found.

The change of peaks on ^{15}N-^{1}H heteronuclear single quantum coherence (HSQC) spectra of RpsA (280-438) and its ligands is concluded in Figure 5, and Figure 5a shows the spectrum of RpsA (280-438) and PXYC1. As

shown in Figure 5b-5 g, for each compound, some peaks move and some peaks become broader. In solution, proteins and ligands form an exchanging system, where ligands bind to or unbind from proteins. When ligands show low affinity, the peaks from the nearby amino acids move due to the fast unbinding of the ligand. For ligands with high affinity, the peaks get broader because the back reaction of binding is slower than the frequency difference between the bound and free proteins[30]. The broader peaks shown in Figure 5 mean that the compounds have a high affinity for RpsA (280-438), which is in consistent with the K_d values given by FQT. More importantly, considering moving and broader peaks, the visualized binding sites of the active compounds correspond to the sites for *in silico* design (Figure 6). The PXYC1, PXYC2, PXYC12 and PXYC13 sites are around the β-strand barrel that binds RNA. These four strong compounds may compete with RNA. The PXYD3 and PXYD4 sites are between an α-helix and the β-strand barrel, so they may be successful allosteric inhibitors. Though the idea of allosteric inhibitors needs further validation based on biological tests, their high affinity makes them chemical tools for further evaluation. Based on these facts, compounds with high affinities were successfully designed.

(a)

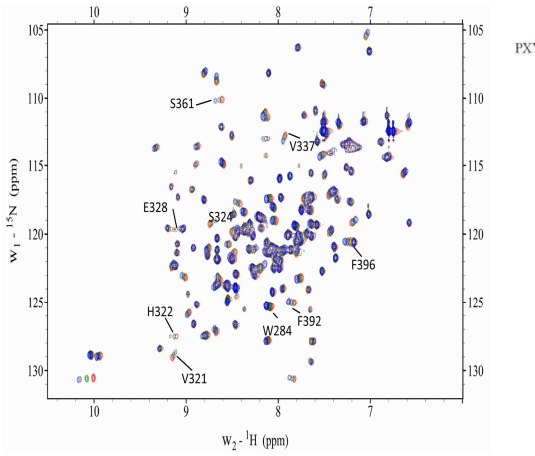
S361
V337
E328
S324
F396
H322
W284
F392
V321
w_1 - ^{15}N (ppm)
w_2 - ^{1}H (ppm)

(b)

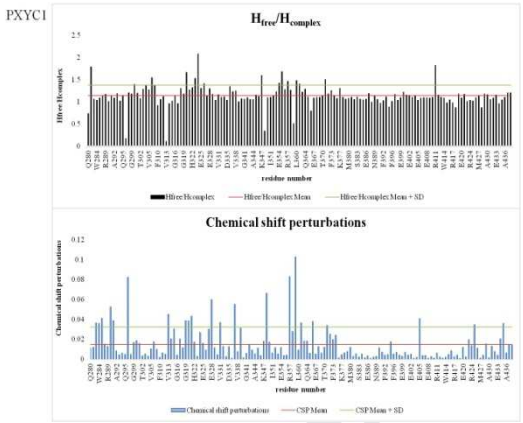
PXYC1
$H_{free}/H_{complex}$
Chemical shift perturbations
residue number

(c)

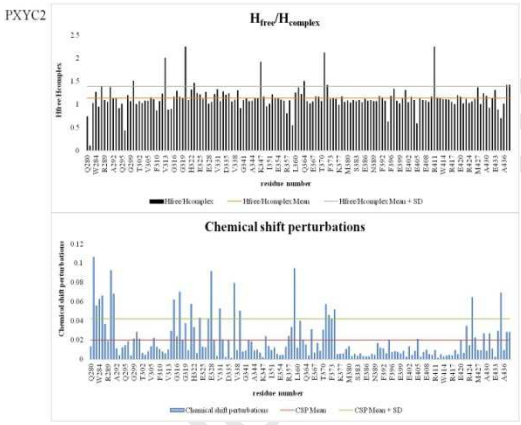
PXYC2
$H_{free}/H_{complex}$
Chemical shift perturbations
residue number

(d)

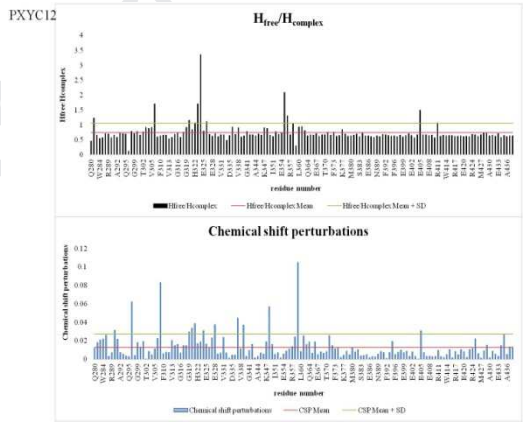
PXYC12
$H_{free}/H_{complex}$
Chemical shift perturbations
residue number

(e)

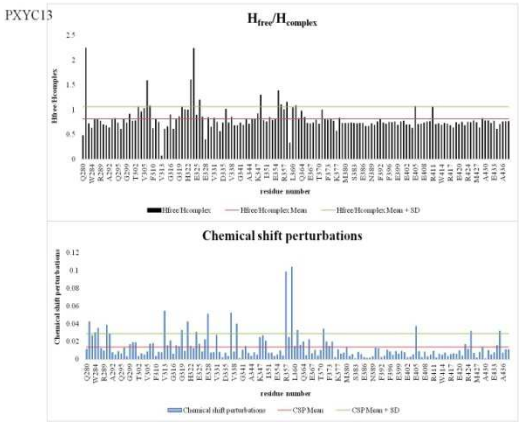
PXYC13
$H_{free}/H_{complex}$
Chemical shift perturbations
residue number

(f)

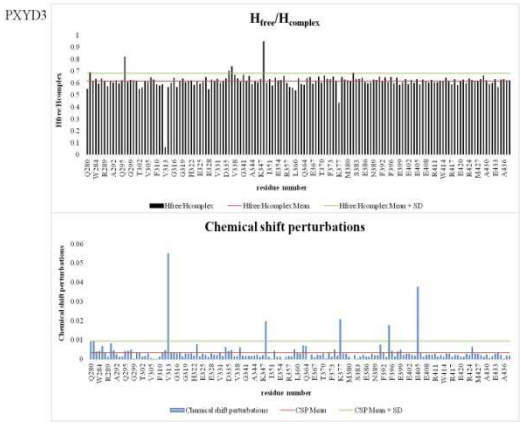
PXYD3
$H_{free}/H_{complex}$
Chemical shift perturbations
residue number

(g)

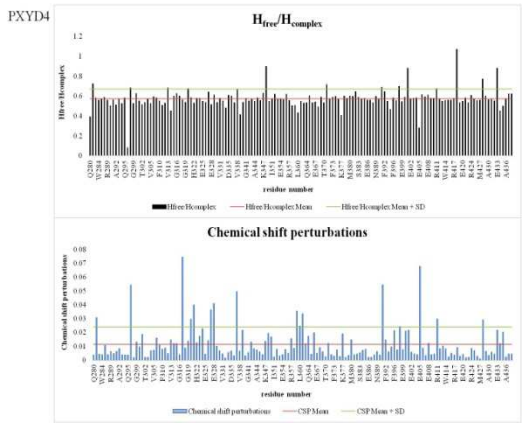

Figure 5. Results of the CSP experiments. (a) Superimposed spectrum of PXYC1. The peaks in red, green and blue represent compound/protein ratios of 1, 5 and 15, respectively. (b-g) Quantitative descriptions for changes in the spectra belonging to PXYC1, PXYC2, PXYC12, PXYC13, PXYD3 and PXYD4, respectively. $H_{free}/H_{complex}$ describes the changes in intensity, and chemical shift perturbation describes the movement of peaks. In each figure, the lower horizontal line represents the mean value of the corresponding changes, and the upper horizontal line represents the mean value plus the corresponding standard deviation. Change values larger than the upper horizontal line indicate significant changes.

(a) (b)

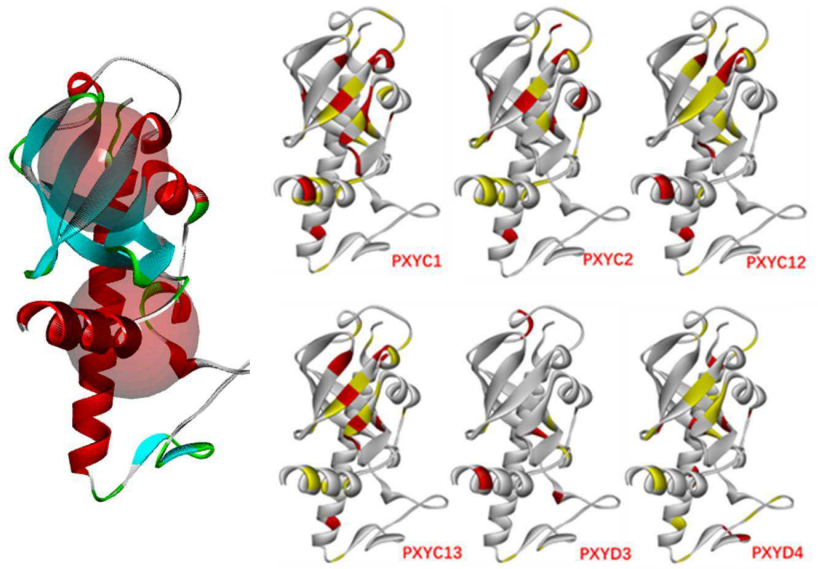

Figure 6. Binding sites. (a) Predefined binding sites for molecular docking. The two spheres are binding sites. The site near the blue β-strands was used to design the PXYC series, and the other site was used to design the PXYD series. (b) Binding sites determined by the CSP experiments. Amino acids with shifts in the spectra are in yellow, while amino acids with broader peaks are in red.

Conclusion

Based on the complex structure of POA and RpsA-CTD, 17 compounds were screened and synthesized. With STD experiments, six compounds were found to have effects on both RpsA-CTD and RpsA-CTD Δ438A, and these interactions were further proven by FQT. The FQT experiments also helped to determine the K_d values between each protein and the active compounds, of which PXYC1 showed the highest affinity. The

SAR analysis of the PXYC and PXYD series can help design compounds with higher affinity, and thus, better lead compounds for treating tuberculosis may be further developed. Finally, the CSP experiments validate the binding sites of the six compounds. By targeting the trans-translation process of *Mtb*, PXYC1, PXYC2, PXYC12 and PXYC13 provide new leads for treating *Mtb* infections, and their effects on both RpsA-CTD and RpsA-CTD Δ438A may limit antibiotic resistance. In addition, PXYD3 and PXYD4 can be chemical tools to further study the feasibility of allosteric inhibitors of RpsA.

Experimental section

Molecular docking

Based on the complex structure of RpsA-CTD and POA (PDB code: 4NNI) and the structure of RpsA-CTD Δ438A (PDB code: 4NNG)[12], molecular docking was performed by CDocker[30], and CDocker energy and CDocker interaction energy were used as the scoring functions to screen the compound libraries of Antibacterial_5460 and Antivriral_77260 in the ChemDiv commercial library, Drugbank and Zinc. In 4NNI with Arg357 protonated, a coordinate (x=12.681, y=3.955, z=22.145) was set as the centre of a sphere with a radius of 7.0 Å to perform the first round of virtual screening. Then, docking was performed in 4NNG with Arg357 protonated and a coordinate (x=6.065, y=16.396,

z=1.71) and a radius (7.7 Å) were set. Then, the same settings in 4NNI without the protonated Arg357 were used for the next round of screening, followed by screening based on the unprotonated 4NNG, with the following settings: x=-2.291, y=12.954, z=-11.134 and radius=7.0 Å. The compounds having scores better than POA (protonated model: -CDocker_energy > 20, -CDocker_interaction_energy > 30; unprotonated model: -CDocker_energy > 8, -CDocker_interaction_energy > 22) were selected. For the allosteric site, the coordinates (x=-6.553 y= -11.292 z=27.764) and (x=-8.378 y= -5.605 z=1.888) were set for 4NNI and 4NNG, respectively, and radii of 8.1 Å and 8.2 Å, respectively, were set tentatively. Antibacterial_5460 and Antivriral_77260 in the ChemDiv commercial library and Drugbank were screened, and the compounds with higher -CDocker energy and -CDocker interaction energy were preferred.

Synthesis

Ethyl cyanoacetate was purchased from Energy Chemical (Shanghai, China). Chloroacetyl chloride and ethyl chloroacetate were purchased from Shaoyuan Technology (Shanghai, China). Reagents commonly used in the laboratory were all chemically pure. The ^{1}H and ^{13}C NMR spectra were collected with Bruker Avance 300 or 850 MHz spectrometers. High-resolution mass spectra (HRMS) were collected on an Agilent

ESI-TOF mass spectrometer.

Synthesis of the PXYC series

Synthesis of 6-amino-2-mercaptopyrimidin-4(3H)-one (compound 1). The reaction was carried out in a three-necked round bottom flask, using the two side necks for refluxing and purging nitrogen with a dry tube. To the flask, 37.5 mL of absolute ethanol was added, and a sodium block (1.13 g, 49.2 mmol) was slowly added with ice-cooling and magnetic stirring. After the sodium block disappeared, thiourea (3.923 g, 51.5 mmol) was added and the system was purged with nitrogen. Ethyl cyanoacetate (5 mL, 46.9 mmol) was added slowly under the nitrogen atmosphere. Initially, a yellow solid started to precipitate and finally the solution clarified. Then, a large amount of white solid appeared, and the reaction stirred at 75 °C for 2 h. The white solid was obtained and then dissolved in water (35 mL). The pH of the solution was adjusted to 4 with acetic acid, and the white precipitate was separated by filtration and washed with ethyl acetate and petroleum ether to obtain a white solid (5.84 g, 87%). ^{1}H NMR (300 MHz, DMSO-d6) δ 11.64 (s, 1H), 11.54 (s, 1H), 6.38 (s, 2H), 4.69 (s, 1H).

Synthesis of 6-amino-2-mercapto-5-nitrosopyrimidin-4(3H)-one (compound 2). Compound 1 (0.5 g, 3.5 mmol) was dissolved in a solution of 8.93 mL water and 1.8 mL acetic acid. At the same time, 0.446 g (6.5

mmol) of sodium nitrite was dissolved in 1.4 mL of water. In an ice bath, the aqueous sodium nitrite solution was slowly added to the compound 1 solution with stirring. During the addition, the solution gradually turned brick red. After 16 h of stirring at room temperature, the mixture was filtered and the filter cake was washed with water and ethanol to give a brick red solid (0.45 g, 76%). As the compound has only active hydrogens, we have listed only its ^{13}C NMR spectrum. ^{13}C NMR (75 MHz, DMSO-d6) δ 140.38, 142.60, 159.38, 176.43.

Synthesis of 5,6-diamino-2-mercaptopyrimidin-4(3H)-one (compound 3). Compound 2 (0.45 g, 2.6 mmol) was dissolved in 10.56 mL aqueous saturated sodium bicarbonate. Sodium dithionite (1.366 g, 7.8 mmol) was slowly added to the reaction solution in an ice bath. The reaction stirred for 7 h, during which the solution turned from blood red to pale yellow and then white. After the reaction was complete, the pH of the solution was adjusted to 5 with acetic acid, and the solution was placed in a refrigerator for a few minutes. The solution was filtered and the filter cake was washed with water and ethanol to give a white solid (0.369 g, 89%). ^{1}H NMR (300 MHz, DMSO-d6) δ 5.68 (br, 6H); ^{13}C NMR (75 MHz, DMSO-d6) δ 102.43, 104.56, 157.86, 167.45.

Synthesis of N-(4-amino-2-mercapto-6-oxo-1,6-dihydropyrimidin-5-yl)

formamide (compound 4). Compound 3 (2.85 g, 18 mmol) was dissolved in 90% formic acid and the solution stirred at 101 °C for 2 h. During the reaction, a dry tube was added to the reflux device, and formic acid was added to the reaction flask to avoid solidification. After the reaction, the mixture was cooled to 0 °C. The mixture was then filtered and the filter cake was washed and dried to obtain a pale yellow solid (3.16 g, crude yield: 94%).

Synthesis of 2-thioxanthine (compound PXYC3). Compound 4 (3.16 g, 17 mmol) was dissolved in 8 mL of formamide solution, and the solution was allowed to stir at 178 °C. A large amount of bubbles were generated and there was only a small amount of liquid left in the reaction flask at the end of the reaction. After cooling to room temperature, a filter cake was obtained by filtration, which was then dissolved in 1 M sodium hydroxide, producing a yellow liquid. The solution was decolorized with activated carbon, and the filtrate was retained after filtration. The solution was adjusted to acidic pH with acetic acid, and a yellow solid precipitated. After filtration, the filter cake was washed with ethyl acetate and petroleum ether to give a pale yellow solid (2.36 g). ^{1}H NMR (300 MHz, DMSO-d6) δ 8.05 (s, 1H); ^{13}C NMR (75 MHz, DMSO-d6) δ 110.84, 141.97, 149.32, 153.90, 173.82; HRMS (ESI) m/z $[M+H]^{+}$: 169.0175.

Synthesis of ethyl 2-((6-oxo-6,7-dihydro-1H-purin-2-yl)thio)acetate

(compound PXYC1). To 25 mL of water, PXYC3 (0.44 g, 2.6 mmol) was added and the solution was heated to 70 °C, followed by the addition of 2.5 mL of 1 M sodium hydroxide with stirring. Acetic acid was added to disperse PXYC3 as white granules, and then 560 μl (0.6418 g, 5.2 mmol) of ethyl chloroacetate was added. The reaction was monitored via TLC. After the reaction was complete, the pH of the solution was adjusted to 5 and the solution was filtered. The filter cake was washed with ethanol and ethyl acetate and finally dried in vacuo to yield a white solid (0.42 g). ^{1}H NMR (300 MHz, DMSO-d6) δ 1.19 (t, J = 7.1 Hz, 3H), 4.07 (s, 2H), 4.13 (q, J = 7.1 Hz, 2H), 8.02 (s, 1H), 12.64 (s, 1H), 13.08 (s, 2H); ^{13}C NMR (213MHz, DMSO-d6) δ 14.47, 32.84, 61.66, 141.88, 149.38, 153.99, 168.84, 173.83; HRMS (ESI) m/z $[M+H]^{+}$: 255.0520.

Synthesis of 2-((6-oxo-6,7-dihydro-1H-purin-2-yl)thio)acetic acid (compound PXYC2). PXYC1 (0.42 g, 1.65 mmol) was dissolved in 6 mL of 1 M aqueous sodium hydroxide. The reaction stirred at 70 °C for 2 h, during which the solution became pale yellow. The reaction was monitored via TLC, and the mixture was cooled to room temperature after the reaction was complete. Acetic acid was added to the reaction mixture to precipitate the product as a white solid. The solid was obtained by filtration and dried to give a white solid powder (0.3 g). ^{1}H NMR (300 MHz, DMSO-d6) δ 7.99 (s, 1H), 3.80 (s, 2H); ^{13}C NMR (75 MHz,

DMSO-d6) δ 34.62, 116.65, 139.58, 153.02, 156.03, 155.56, 170.62; HRMS (ESI) m/z $[M+H]^+$: 227.0226.

General procedure for the synthesis of compounds 5-14. The corresponding amine was dissolved in anhydrous dichloromethane at 0 °C, and then triethylamine (1.1 *eq*) was added under a nitrogen atmosphere. Chloroacetyl chloride (1.1 *eq*) diluted with anhydrous dichloromethane was slowly added to the reaction mixture in an ice bath. The reaction stirred at 0 °C for 30 min, after which the reaction slowly warmed to room temperature overnight. TLC was used to monitor the reaction. After the reaction was complete, it was quenched with water and extracted with dichloromethane. The organic phase was retained and washed with an aqueous hydrochloric acid solution, an aqueous saturated sodium hydrogen carbonate solution, and brine three times. Anhydrous sodium sulfate was used to dry the organic phase, after which the solvent was removed under reduced pressure with a rotary evaporator to obtain crude product. The crude product was dissolved in ethyl acetate and recrystalized with petroleum ether to afford the final product. Compounds 5-14 were in 58-86% yield.

2-chloro-N-phenylacetamide (compound 5). ^{1}H NMR (300 MHz, DMSO-d6) δ 4.26 (s, 2H), 7.10 (t, J = 7.4 Hz, 1H), 7.34 (t, J = 8.0 Hz,

2H), 7.59 (d, J = 7.9 Hz, 2H), 10.30 (s, 1H).

Methyl 4-(2-chloroacetamido)benzoate (compound 6). ^{1}H NMR (300 MHz, DMSO-d6) δ 3.83 (s, 3H), 4.31 (s, 2H), 7.74 (d, J = 8.4 Hz, 2H), 7.95 (d, J = 8.4 Hz, 2H), 10.65 (s, 1H).

2-chloro-N-(3-methoxyphenyl)acetamide (compound 7). ^{1}H NMR (300 MHz, $CDCl_3$) δ 2.34 (s, 3H), 4.16 (s, 2H), 6.98 (d, J = 7.5 Hz, 1H), 7.23 (t, J = 7.8 Hz, 1H), 7.41-7.29 (m, 2H), 8.24 (s, 1H).

2-chloro-N-(thiazol-2-yl)acetamide (compound 8). ^{1}H NMR (300 MHz, $CDCl_3$) δ 5.13 (s, 2H), 7.91 (d, J = 3.5 Hz, 1H), 8.10 (s, 1H), 8.36 (d, J = 3.6 Hz, 1H).

2-chloro-N-phenethylacetamide (compound 9) ^{1}H NMR (300 MHz, $CDCl_3$) δ 2.87 (t, J = 7.0 Hz, 2H), 3.59 (q, J = 6.9 Hz, 2H), 4.04 (s, 2H), 6.65 (s, 1H), 7.41-7.28 (m, 2H), 7.33-7.18 (m, 3H).

N-benzyl-2-chloroacetamide (compound 10). ^{1}H NMR (300 MHz, DMSO-d6) δ 4.12 (s, 2H), 4.51 (d, J = 5.8 Hz, 2H), 6.89 (s, 1H), 7.28 (d, J = 6.0 Hz, 1H), 7.32 (s, 2H), 7.44-7.30 (m, 2H).

2-chloro-N-(2-chlorophenyl)acetamide (compound 11). ^{1}H NMR (300 MHz, $CDCl_3$) δ 4.24 (s, 2H), 7.11 (td, J = 7.7, 1.6 Hz, 1H), 7.41 (dd, J = 8.0, 1.5 Hz, 1H), 7.40-7.23 (m, 1H), 8.37 (dd, J = 8.3, 1.5 Hz, 1H), 8.94 (s, 1H).

2-chloro-N-(3-methylbenzyl)acetamide (compound 12). ^{1}H NMR (300 MHz, $CDCl_3$) δ 1.63 (s, 3H), 4.10 (s, 2H), 4.45 (d, J = 5.8 Hz, 2H), 6.84 (s, 1H), 7.10 (m, 3H), 7.28-7.20 (m, 1H).

2-chloro-N-(4-methylbenzyl)acetamide (compound 13). Used as a crude product for its next reaction.

Ethyl (2-chloroacetyl)glycinate (compound 14). Used as a crude product for its next reaction.

General procedure for the synthesis of compounds PXYC5-PXYC13. To an absolute ethanol solution of the corresponding chloroacetamide derivatives, triethylamine or potassium carbonate (1.2 *eq*) was added, followed by the addition of PXYC3 (1.1 *eq*) at room temperature. The reaction stirred overnight. When the reaction was found to be slow via TLC, the reaction temperature was slowly increased to 50 °C. After the reaction was complete, the solution was acidified by the addition of acetic

acid. Then, the mixture was filtered and the filter cake was washed with water, ethanol and ethyl acetate. A dilute sodium hydroxide solution was added to dissolve the filter cake in an ice bath, and the solution was adjusted to acidic pH to precipitate the corresponding product. After the mixture was filtered, the filter cake was washed with cyclohexane and dried. When the purity was low, purification was performed with column chromatography (DCM:methanol 20:1, triethylamine added). Compounds PXYC5-PXYC13 were in 64-90% yield.

2-((6-oxo-6,7-dihydro-1H-purin-2-yl)thio)-N-phenylacetamide (compound PXYC5). ^{1}H NMR (300 MHz, DMSO-d6) δ 4.17 (s, 2H), 7.30 (t, J = 7.7 Hz, 2H), 7.05 (t, J = 7.4 Hz, 1H), 7.58 (d, J = 8.0 Hz, 2H), 8.05 (s, 1H), 10.36 (s, 1H); ^{13}C NMR (213MHz, DMSO-d6) δ 35.70，119.60，123.94，129.26，139.32，166.18，124.60，130.79，143.70，166.23，166.82; HRMS (ESI) m/z $[M+H]^+$: 302.0675.

Methyl 4-(2-((6-oxo-6,7-dihydro-1H-purin-2-yl)thio)acetamido)benzoate (compound PXYC6). ^{1}H NMR (300 MHz, DMSO-d6) δ 3.81 (s, 3H), 4.20 (s, 2H), 7.72 (d, J = 8.5 Hz, 2H), 7.91 (d, J = 8.4 Hz, 2H), 8.06 (s, 1H), 10.74 (s, 1H), 12.98 (s, 1H); HRMS (ESI) m/z $[M+H]^+$: 360.0734.

N-(3-methoxyphenyl)-2-((6-oxo-6,7-dihydro-1H-purin-2-yl)thio)acetamid

e (compound PXYC7). ^{1}H NMR (300 MHz, DMSO-d6) δ 2.26 (s, 3H), 4.15 (s, 2H), 6.87 (d, J = 7.5 Hz, 1H), 7.18 (t, J = 7.8 Hz, 1H), 7.56-7.26 (m, 2H), 8.07 (s, 0H), 10.27 (s, 1H), 12.59 (s, 1H); ^{13}C NMR (213MHz, DMSO-d6) δ 35.70, 116.79, 120.12, 124.63, 129.09, 138.45, 139.25, 142.06, 166.08, 173.86.

2-((6-oxo-6,7-dihydro-1H-purin-2-yl)thio)-N-(thiazol-2-yl)acetamide (compound PXYC8). ^{1}HNMR (300 MHz, DMSO-d6) δ 4.18 (s, 2H), 7.21 (s, 1H), 7.46 (s, 1H), 7.96 (s, 1H), 12.88 (br, 3H).

2-((6-oxo-6,7-dihydro-1H-purin-2-yl)thio)-N-phenethylacetamide (compound PXYC9). ^{1}H NMR (300 MHz, DMSO-d6) δ 2.70 (t, J = 7.0 Hz, 2H), 3.90 (t, J = 6.9 Hz, 2H), 3.90 (s, 2H), 7.48-7.00 (m, 5H), 8.07 (s, 1H), 8.28 (s, 1H), 12.22 (s, 1H), 13.39 (s, 1H); ^{13}C NMR (213MHz, DMSO-d6) δ 34.45, 35.38, 41.15, 110.72, 126.50, 128.77, 128.70, 129.05, 139.70, 142.06, 149.45, 153.86, 167.37, 173.86; HRMS (ESI) m/z $[M+H]^{+}$: 330.0981.

N-benzyl-2-((6-oxo-6,7-dihydro-1H-purin-2-yl)thio)acetamide (compound PXYC10). ^{1}H NMR (300 MHz, DMSO-d6) δ 4.00 (s, 2H), 4.31 (d, J = 5.9 Hz, 2H), 7.24 (d, J = 13.4 Hz, 5H), 8.06 (s, 1H), 8.68 (s, 1H), 12.16 (s, 1H); ^{13}C NMR (213MHz, DMSO-d6) δ 34.45, 42.95,

127.15, 127.48, 128.68, 139.49, 141.92, 149.38, 167.48; HRMS (ESI) m/z $[M+H]^+$: 316.0832.

N-(2-chlorophenyl)-2-((6-oxo-6,7-dihydro-1H-purin-2-yl)thio)acetamide (compound PXYC11). ^{1}H NMR (300 MHz, DMSO-d6) δ 4.20 (s, 2H), 7.17 (t, J = 7.7 Hz, 1H), 7.32 (t, J = 7.7 Hz, 1H), 7.47 (d, J = 7.9 Hz, 1H), 7.81 (d, J = 8.1 Hz, 1H), 8.14 (s, 1H), 9.86 (s, 1H), 12.64 (s, 1H), 13.40 (s, 1H); ^{13}C NMR (213MHz, DMSO-d6) δ 35.01, 125.63, 126.23, 126.70, 129.89, 127.96, 135.13, 166.97; HRMS (ESI) m/z $[M+H]^+$: 336.0277.

N-(3-methylbenzyl)-2-((6-oxo-6,7-dihydro-1H-purin-2-yl)thio)acetamide (compound PXYC12). ^{1}H NMR (300 MHz, DMSO-d6) δ 2.20 (s, 3H), 3.98 (s, 2H), 4.30-4.21 (m, 2H), 7.01 (s, 3H), 7.13 (s, 1H), 8.06 (s, 1H), 8.66 (s, 1H), 12.19 (s, 0H), 12.56 (s, 1H); ^{13}C NMR (213MHz, DMSO-d6) δ 21.36, 34.45, 42.93, 110.72, 124.67, 128.62, 128.06, 127.82, 137.76, 139.38, 142.06, 149.45, 153.86, 157.49, 167.45, 173.86; HRMS (ESI) m/z $[M+H]^+$: 330.0859.

N-(4-methylbenzyl)-2-((6-oxo-6,7-dihydro-1H-purin-2-yl)thio)acetamide (compound PXYC13). ^{1}H NMR (300 MHz, DMSO-d6) δ 2.24 (s, 3H), 3.98 (s, 2H), 4.24 (d, J = 5.9 Hz, 2H), 7.08 (t, J = 12.4 Hz, 4H), 8.06 (s, 1H), 8.67 (s, 1H), 12.20 (s, 1H); ^{13}C NMR (213MHz, DMSO-d6) δ 21.12,

34.48, 42.73, 110.81, 127.51, 129.23, 136.20, 136.42, 142.01, 149.38, 153.91, 154.31, 167.42, 173.86; HRMS (ESI) m/z $[M+H]^+$: 330.0971.

General procedure for the synthesis of compounds PXYD1-PXYD5. 5,7-Dihydroxyflavone was dissolved in anhydrous DMF, after which potassium carbonate (1.2 *eq*) was added, and the mixture stirred for 1 h, during which the solution became yellow. Then, the corresponding chloroacetamide derivatives (1.2 *eq*) was added, and the reaction stirred at 80 °C for 5 h, during which TLC was used to monitor the reaction. When the reaction was complete, the mixture was poured into cold water, and the pH was adjusted to be acidic. Then, the mixture was extracted with ethyl acetate and the organic phase was retained and washed with brine three times. The organic phase was dried over anhydrous sodium sulfate, and then the solvent was removed under reduced pressure with a rotary evaporator to obtain crude product. The crude product was mixed with silica gel and purified by column chromatography (PE:EA 2:1). Compounds PXYD1-PXYD5 were in 43-80% yield.

2-((5-hydroxy-4-oxo-2-phenyl-4H-chromen-7-yl)oxy)-N-phenethylacetamide (compound PXYD1). ^{1}H NMR (300 MHz, DMSO-d6) δ 2.76 (t, J = 7.4 Hz, 2H), 3.49 (q, 2H), 4.63 (s, 2H), 6.44 (d, J = 2.2 Hz, 1H), 6.80 (d, J = 2.3 Hz, 1H), 7.07 (s, 1H), 7.32-7.10 (m, 5H), 7.61 (q, J = 6.7, 6.2 Hz, 3H),

8.15-8.05 (m, 2H), 8.26 (t, J = 5.5 Hz, 1H), 12.82 (s, 1H); ^{13}C NMR (213MHz, DMSO-d6) δ 35.49, 40.46, 67.67, 93.99, 99.31, 105.76, 105.90, 126.52, 126.92, 128.73, 129.06, 129.62, 131.02, 132.65, 139.71, 157.65, 161.56, 164.09, 164.02, 167.15, 182.56; HRMS (ESI) m/z $[M+H]^+$: 416.1462.

N-(2-chlorophenyl)-2-((5-hydroxy-4-oxo-2-phenyl-4H-chromen-7-yl)oxy) acetamide (compound PXYD2). ^{1}H NMR (300 MHz, DMSO-d6) δ 4.74 (s, 2H), 6.50 (d, J = 2.3 Hz, 1H), 6.61 (t, J = 2.6 Hz, 1H), 6.72 (s, 1H), 7.10 (td, J = 7.7, 1.6 Hz, 1H), 7.39-7.26 (m, 1H), 7.41 (dd, J = 8.0, 1.5 Hz, 1H), 7.62-7.47 (m, 4H), 7.96-7.85 (m, 2H), 8.93 (s, 1H), 12.82 (s, 1H); ^{13}C NMR (213MHz, DMSO-d6) δ 67.65, 94.22, 95.38, 99.26, 105.85, 105.94, 126.37, 126.95, 127.02, 127.29, 128.12, 129.66, 130.03, 130.97, 131.03, 132.70, 134.53, 157.69, 161.75, 164.03, 164.10, 166.55, 182.61.

2-((5-hydroxy-4-oxo-2-phenyl-4H-chromen-7-yl)oxy)-N-(3-methylbenzyl) acetamide (compound PXYD3). ^{1}H NMR (300 MHz, $CDCl_3$) δ 2.32 (s, 3H), 4.53 (d, J = 5.8 Hz, 2H), 4.62 (s, 2H), 6.39 (d, J = 2.2 Hz, 1H), 6.52 (d, J = 2.3 Hz, 1H), 6.69 (s, 1H), 6.79 (s, 1H), 7.09 (d, J = 6.0 Hz, 3H), 7.23 (s, 1H), 7.64-7.46 (m, 3H), 7.88 (dd, J = 7.5, 1.9 Hz, 2H), 12.75 (s, 1H); ^{13}C NMR (213MHz, DMSO-d6) δ 21.22, 42.26, 67.68, 94.02, 99.40, 105.75, 105.88, 126.89, 128.57, 130.99, 124.82, 137.76, 128.22, 139.54,

132.65, 129.60, 127.87, 157.63, 161.56, 164.01, 164.12, 167.34, 170.78, 182.54; HRMS (ESI) m/z $[M+H]^+$: 416.1471.

2-((5-hydroxy-4-oxo-2-phenyl-4H-chromen-7-yl)oxy)-N-(4-methylbenzyl) acetamide (compound PXYD4). ^{1}H NMR (300 MHz, DMSO-d6) δ 2.15 (s, 3H), 3.99 (s, 2H), 4.14 (d, J = 5.9 Hz, 2H), 6.11 (d, J = 2.1 Hz, 1H), 6.41 (d, J = 2.1 Hz, 1H), 6.84 (s, 1H), 7.16-6.95 (m, 4H), 7.55-7.38 (m, 3H), 7.94 (dt, J = 6.6, 1.8 Hz, 2H), 8.57 (s, 1H), 12.72 (s, 1H); ^{13}C NMR (213MHz, DMSO-d6) δ 21.12, 43.12, 67.69, 94.58, 99.49, 104.44, 105.64, 126.86, 127.73, 127.78, 129.22, 129.32, 129.59, 131.18, 132.46, 136.25, 136.32, 136.47, 136.61, 157.92, 161.94, 163.62, 164.91, 166.35, 182.3; HRMS (ESI) m/z $[M+H]^+$: 416.1447.

Ethyl(2-((5-hydroxy-4-oxo-2-phenyl-4H-chromen-7-yl)oxy)acetyl)glycinat e (compound PXYD5). ^{1}H NMR (300 MHz, $CDCl_3$) δ 1.32 (t, J = 7.1 Hz, 3H), 4.16 (d, J = 5.3 Hz, 2H), 4.27 (q, J = 7.1 Hz, 2H), 4.64 (s, 2H), 6.45 (d, J = 2.3 Hz, 1H), 6.58 (d, J = 2.3 Hz, 1H), 6.72 (s, 1H), 7.05 (s, 1H), 7.56 (d, J = 7.1 Hz, 3H), 7.91 (d, J = 7.0 Hz, 2H), 12.79 (s, 1H); ^{13}C NMR (213MHz, DMSO-d6) δ 14.52, 40.99, 61.01, 67.51, 94.13, 99.39, 105.81, 105.92, 126.93, 129.64, 131.02, 132.69, 157.67, 161.55, 164.03, 164.06, 167.98, 170.01, 182.59; HRMS (ESI) m/z $[M+H]^+$: 398.1213.

Protein expression and purification. RpsA-CTD (285-476) and RpsA-CTD Δ438A (285-476) were prepared as described before[4]. ^{15}N-labelled wild-type RpsA (280-438) was prepared as described previously[29].

STD experiments. The proteins were dissolved in 10 mM PBS 6.0 solution containing 150 mM NaCl, and the compounds were dissolved in DMSO-d6 with a concentration of 100 mM. A solution containing 500 μL of 20 μM RpsA-CTD or RpsA-CTD Δ438A, 500 μM compound and 10% D_2O was prepared, and the solution was added to an NMR tube. A Bruker Advance 850 MHz spectrometer was used to perform the STD experiments. The saturation frequency for difference spectra was set at -800 Hz, while the frequency for reference spectra was set at 42500 Hz. The collected data was processed with Bruker Topspin 3.2.

FQT experiments. The Stern-Volmer equation was first used to determine whether quenching was static[26]:

$$F_0/F = 1+ K_q\tau_0[Q].$$

In this equation, F_0 and F are the fluorescence intensity before and after the addition of quenching agent, respectively, [Q] is the concentration of quenching agent and τ_0 is the fluorescence lifetime, whose average value

for biomacromolecules is 1×10^{-8} sec. With these values, the quenching rate constant (K_q) can be calculated, and a K_q value larger than 2.0×10^{10} M^{-1} sec^{-1} indicates static quenching.

The dissociation constant (K_d) and the number of binding sites (n) were then calculated by the double logarithm regression curve[27]:

$$\log[(F_0\text{-}F)/F] = \log K_a + n\log[Q].$$

In this equation, K_a is the binding constant, and K_d is the reciprocal of K_a.

For FQT experiments, 100 mM compound solutions in DMSO and 10 mM protein solutions in PBS 6.0 containing 150 mM NaCl were prepared. Then, 200 μL of a solution containing a compound, 17% DMSO and 20 μM of RpsA-CTD or RpsA-CTD Δ438A was prepared. The concentrations of the compounds were 0 μM, 5 μM, 10 μM, 20 μM, 30 μM, 40 μM, 50 μM, 70 μM, 80 μM, 90 μM, 110 μM, 130 μM, 150 μM, 160 μM, 170 μM, 250 μM, 350 μM or 500 μM. POA was used as a control. An F-7000 fluorescence spectrophotometer (HITACHI, Japan) was used to obtain the fluorescence intensity at 330 nm. For each group of one protein and one compound, the determination of fluorescence intensity was repeated three times, and the average intensity was used to calculate the K_d value.

CSP experiments. One hundred millimolar compound solution in DMSO-d6 and a 10 mM protein solution in PBS 6.0 containing 150 mM NaCl were prepared. Then, 500 μL of a solution was added to an NMR tube, which contained 200 μM of ^{15}N-labelled RpsA (280-438) and 10% D_2O. The ^{1}H-^{15}N HSQC spectra were acquired on a Bruker Avance 850 MHz spectrometer at 25 °C. Before acquisition, compound in DMSO-d6 was added to the NMR tube, and the solution was mixed.

The volume of the added PXYC2 solution was 0 μL, 1 μL, 1 μL, 3 μL, 2 μL and 8 μL. The volumes for PXYC1 were 0 μL, 1 μL, 1 μL, 3 μL and 2 μL, while the volumes for PXYC12, PXYC13, PXYD3 and PXYD4 were 0 μL, 1 μL, 1 μL and 3 μL. Equivalent volumes of DMSO-d6 containing no compound were used as controls to deduct the interference of DMSO-d6.

The moving of peaks belonging to acylamide groups ($\Delta\delta$ N–H) were calculated by the following equation[30, 32]:

$$\Delta\delta \text{ N–H} = ((\Delta\delta \text{ H})^2 + (\Delta\delta \text{ N}/5)^2)^{1/2}.$$

In this equation, $\Delta\delta$ H and $\Delta\delta$ N represent the chemical shift changes of the protons and nitrogens belonging to the acylamide group, respectively.

The broadening of peaks belonging to acylamide groups was described as the intensity changes of the peaks (IPI):

$$IPI = H_{free}/ H_{bind}.$$

Here, H_{bind} and H_{free} represent the height of the peaks in the presence and absence of compound, respectively.

The acquired data was first processed by the NMRpipe[33] software package, and the chemical shifts and intensity values were obtained with Sparky[34].

Acknowledgements

We would like to thank Liubin Feng and Dr. Hongwei Yao from High-Field Nuclear Magnetic Resonance Research Center, Xiamen University for NMR technique support. We thank Dr. Xinli Liao from College of Chemistry and Chemical Engineering, Xiamen University for helpful discussions. We also appreciate the English editing service provided by American Journal Experts.

This work was supported by funds from the National Natural Science Foundation of China, China (81573348) and the "Double First-Class" University Project, China (CPU2018GY15).

References

[1] B.R. Bloom, R. Atun, T. Cohen, C. Dye, H. Fraser, G.B. Gomez, G. Knight, M. Murray, E. Nardell, E. Rubin, J. Salomon, A. Vassall, G. Volchenkov, R. White, D. Wilson, P. Yadav, Tuberculosis, in: Major Infectious Diseases, Washington (DC), 2017.

[2] N.S. Ramadoss, J.N. Alumasa, L. Cheng, Y. Wang, S. Li, B.S. Chambers, H. Chang, A.K. Chatterjee, A.

Brinker, I.H. Engels, K.C. Keiler, Small molecule inhibitors of trans-translation have broad-spectrum antibiotic activity, Proc. Natl. Acad. Sci. U.S.A. 110 (2013) 10282-10287.
[3] J.N. Alumasa, P.S. Manzanillo, N.D. Peterson, T. Lundrigan, A.D. Baughn, J.S. Cox, K.C. Keiler, Ribosome rescue inhibitors kill actively growing and nonreplicating persister Mycobacterium tuberculosis cells, ACS Infect. Dis. 3 (2017) 634-644.
[4] Y. Zhi, Y. Dai, J. Yang, S. Tan, D. Lin, K. Lin, Lead compounds and key residues of ribosomal protein S1 in drug-resistant Mycobacterium tuberculosis, Bioorg. Chem. 82 (2019) 58-67.
[5] W. Shi, X. Zhang, X. Jiang, H. Yuan, J.S. Lee, C.E. Barry, 3rd, H. Wang, W. Zhang, Y. Zhang, Pyrazinamide inhibits trans-translation in Mycobacterium tuberculosis, Science 333 (2011) 1630-1632.
[6] E. Hajnsdorf, I.V. Boni, Multiple activities of RNA-binding proteins S1 and Hfq, Biochimie 94 (2012) 1544-1553.
[7] E.L. Nuermberger, M.K. Spigelman, W.W. Yew, Current development and future prospects in chemotherapy of tuberculosis, Respirology 15 (2010) 764-778.
[8] I.M. Rosenthal, M. Zhang, K.N. Williams, C.A. Peloquin, S. Tyagi, A.A. Vernon, W.R. Bishai, R.E. Chaisson, J.H. Grosset, E.L. Nuermberger, Daily dosing of rifapentine cures tuberculosis in three months or less in the murine model, PLoS Med. 4 (2007) e344.
[9] R. Tasneen, S. Tyagi, K. Williams, J. Grosset, E. Nuermberger, Enhanced bactericidal activity of rifampin and/or pyrazinamide when combined with PA-824 in a murine model of tuberculosis, Antimicrob. Agents Chemother. 52 (2008) 3664-3668.
[10] E. Nuermberger, S. Tyagi, R. Tasneen, K.N. Williams, D. Almeida, I. Rosenthal, J.H. Grosset, Powerful bactericidal and sterilizing activity of a regimen containing PA-824, moxifloxacin, and pyrazinamide in a murine model of tuberculosis, Antimicrob. Agents Chemother. 52 (2008) 1522-1524.
[11] K. Andries, P. Verhasselt, J. Guillemont, H.W. Gohlmann, J.M. Neefs, H. Winkler, J. Van Gestel, P. Timmerman, M. Zhu, E. Lee, P. Williams, D. de Chaffoy, E. Huitric, S. Hoffner, E. Cambau, C. Truffot-Pernot, N. Lounis, V. Jarlier, A diarylquinoline drug active on the ATP synthase of Mycobacterium tuberculosis, Science 307 (2005) 223-227.
[12] J. Yang, Y. Liu, J. Bi, Q. Cai, X. Liao, W. Li, C. Guo, Q. Zhang, T. Lin, Y. Zhao, H. Wang, J. Liu, X. Zhang, D. Lin, Structural basis for targeting the ribosomal protein S1 of Mycobacterium tuberculosis by pyrazinamide, Mol. Microbiol. 95 (2015) 791-803.
[13] M.T. Khan, S.I. Malik, A.I. Bhatti, S. Ali, A.S. Khan, M.T. Zeb, T. Nadeem, S. Fazal, Pyrazinamide-resistant mycobacterium tuberculosis isolates from Khyber Pakhtunkhwa and rpsA mutations, J. Biol. Regul. Homeost. Agents 32 (2018) 705-709.
[14] M.T. Khan, A.U. Rehaman, M. Junaid, S.I. Malik, D.Q. Wei, Insight into novel clinical mutants of RpsA-S324F, E325K, and G341R of Mycobacterium tuberculosis associated with pyrazinamide resistance, Comput. Struct. Biotechno. J. 16 (2018) 379-387.
[15] W. Liu, J. Chen, Y. Shen, J. Jin, J. Wu, F. Sun, Y. Wu, L. Xie, Y. Zhang, W. Zhang, Phenotypic and genotypic characterization of pyrazinamide resistance among multidrug-resistant Mycobacterium tuberculosis clinical isolates in Hangzhou, China, Clin. Microbiol. Infect. 24 (2018) 1016.e1-1016.e5.
[16] A. Singh, P. Somvanshi, A. Grover, Pyrazinamide drug resistance in RpsA mutant (438A) of Mycobacterium tuberculosis: Dynamics of essential motions and free-energy landscape analysis, J. Cell. Biochem. 120 (2018) 7386-7402.
[17] Y. Fan, Y. Dai, M. Hou, H. Wang, H. Yao, C. Guo, D. Lin, X. Liao, Structural basis for ribosome protein S1 interaction with RNA in trans-translation of Mycobacterium tuberculosis, Biochem. Biophys. Res. Commun. 487 (2017) 268-273.

[18] P. Salah, M. Bisaglia, P. Aliprandi, M. Uzan, C. Sizun, F. Bontems, Probing the relationship between Gram-negative and Gram-positive S1 proteins by sequence analysis, Nucleic Acids Res. 37 (2009) 5578-5588.
[19] Y. Zhang, W. Shi, W. Zhang, D. Mitchison, Mechanisms of pyrazinamide action and resistance, Microbiol. Spectr. 2 (2013) 1-12.
[20] A. Viegas, J. Manso, F.L. Nobrega, E.J. Cabrita, Saturation-Transfer Difference (STD) NMR: A simple and fast method for ligand screening and characterization of protein binding, J. Chem. Educ. 88 (2011) 990-994.
[21] A. Gimeno, L.M. Santos, M. Alemi, J. Rivas, D. Blasi, E.Y. Cotrina, J. Llop, G. Valencia, I. Cardoso, J. Quintana, G. Arsequell, J. Jimenez-Barbero, Insights on the Interaction between Transthyretin and Abeta in Solution. A saturation transfer difference (STD) NMR analysis of the role of iododiflunisal, J. Med. Chem. 60 (2017) 5749-5758.
[22] K.J. Yong, T.M. Vaid, P.J. Shilling, F.J. Wu, L.M. Williams, M. Deluigi, A. Pluckthun, R.A.D. Bathgate, P.R. Gooley, D.J. Scott, Determinants of ligand subtype-selectivity at alpha1a-adrenoceptor revealed using saturation transfer difference (STD) NMR, ACS Chem. Biol. 13 (2018) 1090-1102.
[23] M.J. Harner, L. Mueller, K.J. Robbins, M.D. Reily, NMR in drug design, Arch. Biochem. Biophys. 628 (2017) 132-147.
[24] Y. Mu, J. Lin, R. Liu, Interaction of sodium benzoate with trypsin by spectroscopic techniques, Spectrochim. Acta. A Mol. Biomol. Spectrosc. 83 (2011) 130-135.
[25] H. Zhou, S. Bi, Y. Wang, T. Zhao, Characterization of the binding of paylean and DNA by fluorescence, UV spectroscopy and molecular docking techniques, Luminescence 31 (2016) 1013-1019.
[26] L.R. Lakowicz, Principles of Fluorescence Spectroscopy, third ed., Springer, Boston, MA, 2006.
[27] X.L. Wei, J.B. Xiao, Y. Wang, Y. Bai, Which model based on fluorescence quenching is suitable to study the interaction between trans-resveratrol and BSA?, Spectrochim. Acta. A Mol. Biomol. Spectrosc. 75 (2010) 299-304.
[28] S.B. Shuker, P.J. Hajduk, R.P. Meadows, S.W. Fesik, Discovering high-affinity ligands for proteins: SAR by NMR, Science, 274 (1996) 1531-1534.
[29] J. Fu, B. Huang, D. Lin, X. Liao, Chemical shift assignments of Ribosomal protein S1 from Mycobacterium tuberculosis, Biomol. NMR Assign. 11 (2017) 133-136.
[30] M.P. Williamson, Using chemical shift perturbation to characterise ligand binding, Prog. Nucl. Magn. Reson. Spectrosc. 73 (2013) 1-16.
[31] D.S.M.E. Dassault Systèmes BIOVIA, Release 2017, San Diego: Dassault Systèmes, 2016.
[32] P. Aliprandi, C. Sizun, J. Perez, F. Mareuil, S. Caputo, J.L. Leroy, B. Odaert, S. Laalami, M. Uzan, F. Bontems, S1 ribosomal protein functions in translation initiation and ribonuclease RegB activation are mediated by similar RNA-protein interactions: an NMR and SAXS analysis, J. Biol. Chem. 283 (2008) 13289-13301.
[33] F. Delaglio, S. Grzesiek, G.W. Vuister, G. Zhu, J. Pfeifer, A. Bax, NMRPipe: a multidimensional spectral processing system based on UNIX pipes, J. Biomol. NMR 6 (1995) 277-293.
[34] W. Lee, M. Tonelli, J.L. Markley, NMRFAM-SPARKY: enhanced software for biomolecular NMR spectroscopy, Bioinformatics 31 (2015) 1325-1327.

Declaration of interests

☑ The authors declare that they have no known competing financial interests or personal relationships that could have appeared to influence the work reported in this paper.

☐The authors declare the following financial interests/personal relationships which may be considered as potential competing interests: